RSC Advances

ROYAL SOCIETY OF CHEMISTRY

www.rsc.org/advances

An investigation on the influence of support type for Ni catalysed vapour phase hydrogenation of aqueous levulinic acid to γ-valerolactone

Velisoju Vijay Kumar[a,b], Gutta Naresh[a,b], Medak Sudhakar[a], Chatla Anjaneyulu[a], Suresh Kumar Bhargava[b], James Tardio[b], Vanga Karnakar Reddy[c], Aytam Hari Padmasri[c] and Akula Venugopal[a,*]

[a] Catalysis laboratory, I & PC Division, CSIR - Indian Institute of Chemical Technology, Uppal Road, Hyderabad, Telangana - 500 007 India.

*Corresponding author E-mail: akula@iict.res.in Tel: +91-40-27193165; Fax: +91-40-27160921.

[b] Centre for Advanced Materials & Industrial Chemistry (CAMIC), School of Applied Sciences, RMIT University, Melbourne - 3001, Australia.

[c] Department of Chemistry, University College for Women, Osmania University, Koti, Hyderabad - 500 095, Telangana, India.

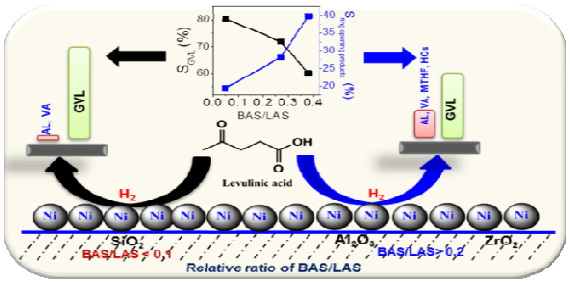

Product distribution is dependent on the nature and strength of acid site in the vapour phase hydrogenation of levulinic acid

Abstract

The 20wt% Ni supported on SiO_2, γ-Al_2O_3 and ZrO_2 catalysts were examined for hydrogenation of aqueous levulinic acid (LA) to γ-Valerolactone (GVL) at 270 °C and ambient pressure. The band intensities of Brønsted (BAS: 1540 cm^{-1}) and Lewis acid sites (LAS: 1450 cm^{-1}) estimated by pyridine adsorbed DRIFT spectra revealed a low ratio of BAS/LAS over the Ni/SiO_2 catalyst than the Ni/ZrO_2 and Ni/γ-Al_2O_3 catalysts. The rate of **angelica lactone** (AL) was lower than the rate of AL hydrogenation over the Ni/SiO_2 catalyst. The poisoning and regeneration of the Ni/SiO_2 catalyst using pyridine and 2,6-dimethylpyridine demonstrated that Lewis acid sites influenced the conversion of LA to AL and subsequent hydrogenation of AL to GVL was occurred on surface Ni site. In contrast Brønsted acid sites were responsible for the ring opening of GVL to **valeric acid (VA)**. Kinetic data emphasized that the hydrogenation activity and product distribution was dependent on the type of acid site and the Ni sites in close proximity to Brønsted acid sites are prone to hydrogenolysis of GVL to valeric acid and hydrocarbons.

Key words: Levulinic acid; Hydrogenation; γ-valerolactone; Pyridine-IR; Brønsted -Lewis acid site; Catalyst self poisoning

1. Introduction

The conversion of levulinic acid (LA), a compound that is obtained from inedible, woody biomass feedstock, namely lignocellulose to fuels and fine chemicals has been a topic of increasing interest.[1,2] In order to achieve the LA to fuels, the first step required is to convert LA to γ-valerolactone (GVL). This can be done via catalytic dehydration of LA to angelica lactone (AL) followed by subsequent catalytic hydrogenation of AL gives rise to GVL. The GVL produced can then be converted to a range of valuable compounds (Scheme 1).

Numerous studies have been conducted on the catalytic hydrogenation of LA to GVL and also the catalytic conversion of GVL to valuable products.[3-7] The majority of the aforesaid studies have been reported in the liquid phase with very few studies being examined in the vapour-phase.[8-14] Zhang et al have reported the selective hydrogenation of LA to GVL in methanol over magnetic $Ni_{4.59}Cu_1Mg_{1.58}Al_{1.96}Fe_{0.70}$ catalyst with a GVL yield of 98.1% at 142 °C.[15] Yan et al reported 91% GVL yield at 200 °C and 70 bar H_2 pressure over Cu based catalysts derived from hydrotalcite precursors during the LA hydrogenation.[16]

The vapour phase conversion of LA to GVL does however have a number of advantages with respect to the liquid phase process such as having no requirement for high pressure conditions, purification, space-to-time yield productivity, environmental impact and generally a reduced likelihood of catalyst deactivation and also additional benefits in terms of efficiency, safety and waste emission.[17]. Dumesic et al. have investigated the vapour phase conversion of LA to GVL using the carbon supported bimetallic Ru-Sn catalyst with a turnover rate of 0.051 s^{-1} using 2-sec-butyl-phenol as solvent at 180 °C and 35 bar H_2 pressure.[18] Upare et al. studied the vapour phase LA hydrogenation at an ambient pressure and 265 °C over the commercial Ru/C catalyst and achieved 100% LA conversion with 100% GVL selectivity.[19] Earlier we have reported LA hydrogenation over the hydroxyapatite

(HAP) supported metal (Ru, Pt, Pd, Ni, Cu) catalysts in the vapour phase at ambient H_2 pressure and 275 °C with 92 % conversion and 99.8% GVL selectivity over the Ru/HAP catalyst.[20]

Although the studies on Ru based catalysts have led to promising results, there is scope for development of cheaper catalysts such as those based on transition metals. Upare et al. have investigated the conversion of aqueous LA to GVL using a Ni promoted copper-silica nano composite catalyst in the presence of formic acid.[21] Mohan et al. examined the Ni/H-ZSM-5 catalyst for LA to GVL at 250 °C and 1 bar H_2 pressure with 100% LA conversion and 92.2% selectivity to GVL.[22] Mechanism of hydrogenation of LA to GVL occurs via either dehydration to angelica lactone followed by its reduction or via reduction of LA to 4-hydroxyvaleric acid and subsequent dehydration. For both of these routes an active metal combined with an acid site should be present on the catalyst surface. It has been reported that Brønsted acid sites are more prone to ring opening of GVL to valeric acid (VA: another fuel additive) and hydrocarbons.[23,24]

However, studies pertaining to support effect for the vapour phase hydrogenation of LA to GVL have not been investigated in detail except recent interesting reports from Weckhuysen group over supported Ru catalysts at high pressures.[25,26] Particularly influence of acid-base characteristics of the various conventional and non-conventional supports such as γ-Al_2O_3, SiO_2, ZrO_2, TiO_2, MgO, ZnO, La_2O_3, hydroxyapatite and carbon as supports for either noble metals or base metals were not explored for the vapour phase conversion of LA to GVL. Our continued activities on the selective hydrogenation of LA to GVL over Ru based catalysts; we have examined several support materials for Ru; for brevity their catalytic activities are given in Table S1 (ESI).[10,20]. Hydrogenation of levulinic acid was also carried out at high H_2 pressures over various noble and non-noble metal catalysts.[27-30] It has been

reported that the nature and type of (Brønsted and/or Lewis) acid site would influence the product distribution during the hydrogenation of levulinic acid.[24]

The present investigation is focussed on the characteristics of the Ni supported on γ-Al_2O_3, SiO_2, and ZrO_2 catalysts; the role of metal site and/or the acid sites would influence the product distribution. The catalysts were characterized by DRIFT analysis and the role of Brønsted and Lewis acid sites are rationalized by poisoning of the catalysts using pyridine and 2,6-dimethylpyridine during the course of reaction. The catalytic activities were evaluated strictly under kinetic regime. Some of the samples were examined by BET-SA, TEM, H_2-TPR and the used catalysts were analysed by CHNS to investigate potential coking.

2. Experimental

2.1 Preparation of catalysts

The SiO_2 (BET-SA: 395.0 m^2 g^{-1}), γ-Al_2O_3 (BET-SA: 230.5 m^2 g^{-1}) ZrO_2 (BET-SA: 52.8 m^2 g^{-1}) $Ni(NO_3)_2 \cdot 6H_2O$, levulinic acid (98%), γ-valerolactone (99%) and angelica lactone (98%), valeric acid, methyl tetrahydrofuran (MTHF) were purchased from Sigma Aldrich and used as received. The α-Al_2O_3 received from NORPRO- R97655. All the catalyst samples were prepared by incipient wet impregnation method. Briefly, required amount of solid support (e.g. SiO_2, γ-Al_2O_3, ZrO_2) and in some case α-Al_2O_3 was added to an aqueous solution of $Ni(NO_3)_2$ $6H_2O$ (an amount required to obtain a 20wt% Ni loading) and the suspension was then stirred at 100 °C until the water had evaporated. The solid recovered was then oven dried at 120 °C overnight and calcined in static air at 500 °C for 5 h.

2.2 Characterization of the catalysts

The powder XRD analysis of the catalysts were recorded with an Ultima-IV X-ray diffractometer (M/s. Rigaku Corporation, Japan) using a Ni-filtered Cu Kα (λ = 0.15418 nm) radiation source and a scintillation counter detector. The diffraction patterns were recorded with a scan rate of 5° min^{-1} in the 2θ range of 10-70° at 40 kV and 20 mA. The average

crystallite size (*D*) of the catalysts was determined by applying Debye-Scherrer equation with respect to the Ni(111) plane. The surface areas of the reduced samples were measured by N_2 adsorption at -196 °C (Micromeritics ASAP 2010 surface area analyzer). The nature of acid sites of the catalysts was examined by pyridine adsorbed FT-IR spectroscopy (Carry 660, Agilent Technologies). Spectra were obtained in the range of 1400-1700 cm^{-1} with a resolution of 2 cm^{-1} with 64 scans for each spectra collection. The experiments were performed in situ using a purpose-made IR cell connected to a vacuum adsorption set-up. In a typical method the reduced samples were pressed into self-supporting wafers (density ~ 40 mg cm^{-3}) under a pressure of 10^5 Pa. Subsequently the wafers were transferred in to the IR cell and were pre-treated in N_2 flow by heating at a rate of 10 °C min^{-1} up to 400 °C for 1 h. After cooling down to 150 °C the spectrum was collected in the drift mode. Then the sample was exposed to pyridine until the surface saturation in successive pulse injections at 150 °C and subsequently the sample was purged for 30 min in N_2 flow before recording the spectra. The drift spectra after pyridine adsorption were subtracted from the spectra of the untreated catalyst to obtain the vibrational bands due to pyridine acid site interaction. Finally, the spectra were quantified with the Kubelka-Munk (K-M) function and the fitted curves were used to measure the relative ratios of Brønsted (BAS) and Lewis acid sites (LAS) for the corresponding spectral lines at full width at half maximum (FWHM). The H_2-TPR analysis was carried out in a quartz micro-reactor interfaced to a gas chromatograph (GC) equipped with a thermal conductivity detector (TCD) unit. Prior to TPR analysis the catalyst was degassed at 300 °C in helium gas for 30 min and then cooled to room temperature. The helium gas was switched to 4.97% H_2 in argon with a flow rate of 30 mL min^{-1} and the temperature was increased to 900 °C at a ramping rate of 5 °C min^{-1}. The hydrogen uptakes of the samples were measured using a calibration curve of Ag_2O TPR under similar protocol. The calibrated mass flow controllers (Alicat Scientific, USA) were used to regulate the flow

rates for all the gases used. Carbon contents in the used samples were measured using a VARIO EL, CHNS analyzer. The elemental analysis of the fresh and used samples were analyzed by atomic absorption spectroscopy (AAS) Perkin-Elmer, Analyst-300. The AAS analysis of the fresh and used samples indicated no leaching of metal during the course reaction (Table S2). The CO pulse chemisorption experiments were carried out using a pulse titration procedure at 40 °C on an AUTOSORB-iQ automated gas sorption analyzer (M/s. Quantachrome Instruments, USA). In a typical method the sample was reductively pre-treated at 450 °C for 2 h in 4.97% H_2 balance Ar then the sample was flushed in helium gas for 30 min at 450 °C followed by titrated with 5.02% CO balance He at 40 °C. The Ni dispersion, Ni metal surface area and particle size of Ni was calculated using the following equations presented below:

$$\text{Dispersion (\%)} = \frac{\text{CO uptake } (\frac{\mu\text{mol}}{g_{cat}})}{\text{Total metal } (\frac{\mu\text{mol}}{g_{cat}})} \times 100$$

$$\text{Metal area} = \text{Metalcross sectional area} \times \text{No. of metal atoms on surface (i. e. CO uptake)}$$

$$\text{Particle size (nm)} = \frac{6000}{\text{Ni metal surface area } \left(\frac{m^2}{g_{cat}}\right) \times \rho}; \ \rho\text{: metal density}$$

2.3 Activity measurements

The vapour phase hydrogenation of aqueous levulinic acid was carried out in a fixed bed quartz reactor (i.d. = 10 mm, length = 420 mm) in down flow mode. The experimental conditions and product analysis details were similar as reported by us earlier.[20] The carbon mass balance in all the experiments were >99% unless otherwise stated. The influence of both Brønsted and Lewis acid sites in the LA conversion was examined by carrying out two independent experiments (1) by using 2,6-dimethylpyridine (2,6-lutidine) as selective Brønsted acid site blocker and (2) pyridine (Py) as both Brønsted and Lewis acid site blocker.

In a typical method about 12.4 mmol of probe was injected successively in 4 pulses (3.1 mmol each) into the aqueous LA stream. After each pulse, the samples were collected and analyzed by GC-MS. After the dosage, the catalyst was regenerated at 450 °C in flowing air and subsequently reduced the catalysts at 450 °C with 4.97% H_2 balance Ar before the aqueous LA was being subjected on to the catalyst. The conversion, selectivity, rates and turnover frequency (TOF) on product formation was calculated using the equations given below:

$$\text{Conversion of LA } (X_{LA}) = \left(\frac{LAc_{in} - LAc_{out}}{LAc_{in}}\right) \times 100$$

$$\text{Selectivity of GVL } (S_{GVL}) = \left(\frac{S_{GVL}}{S_{GVL} + S_{AL} + S_{Others}}\right) \times 100$$

$$\text{Selectivity} = \left[\frac{Pi}{\sum Pi}\right] \times 100 \text{ (where i = GVL, AL and Others)}$$

$$r_{GVL} = \frac{GVL_{yield} \times LA_{flow\ rate}\ (mol\ s^{-1})}{\text{Weight of the catalyst } (g_{cat})}$$

$$TOF = \frac{\text{rate}(mol\ s^{-1} g_{cat}^{-1})}{\text{CO uptake } (mol\ g_{cat}^{-1})}$$

3. Results

3.1 X - ray diffraction and BET - surface area analysis

The XRD patterns of Ni supported on SiO_2, γ-Al_2O_3, and ZrO_2 samples are shown in Fig. 1. Two main diffraction lines appeared at 2θ = 44.5° corresponding Ni (111) plane (ICDD #: 04-0850) and 2θ = 52.0° (Ni (110); ICDD #: 04-0850) is ascribed to metallic Ni phase present in all the samples. The other diffraction lines present in the XRD patterns was due to their respective supports confirmed by ZrO_2 phase (ICDD # 37-1484). The 20wt% Ni/SiO_2 catalyst displayed only a broad peak centred around 2θ = 23° showing micro-crystalline nature of SiO_2. From the previous reports it is clear that because of the close

proximity between Ni, $NiAl_2O_4$ and γ-Al_2O_3 phases, it is difficult to discriminate the isolated phases. However, the formation $NiAl_2O_4$ phase was justified by H_2-TPR analysis of Ni/Al_2O_3 catalyst (Fig.2.). The BET surface area and Ni domain size of 20wt% Ni supported on SiO_2, γ-Al_2O_3, and ZrO_2 catalysts are reported in Table 1. The 20wt% Ni/SiO_2 and 20wt% Ni/γ-Al_2O_3 samples showed significantly higher surface area than the 20wt% Ni/ZrO_2 catalyst. The XRD patterns (Fig. 1.) indicated higher Ni crystallite size on the 20wt% Ni/ZrO_2 (37.8 nm), while the 20wt% Ni/SiO_2 and 20wt% Ni/γ-Al_2O_3 catalysts both had a domain size of Ni ~21 nm. The crystallite size obtained for the respective catalysts indicating that lower the surface area of the support, the extent of Ni agglomeration is higher, as a result large sized Ni particles are formed during the preparation (Table 1).

3.2 H_2 - Temperature programmed reduction (TPR)

The H_2-TPR profiles of 20wt%Ni supported on SiO_2, ZrO_2 and γ-Al_2O_3 catalysts presented in Fig. 2. and their H_2 uptakes are reported in Table 1. The reduction maxima (T_{max}) were different for all the catalysts, although the samples have constant Ni loading. Thus suggests the variation in the Ni interaction with varied supports. The reduction signals appeared in TPR patterns is associated with NiO reduction to Ni^0. For the 20wt% Ni/SiO_2 sample, T_{max} found at 322 °C is an indication of dispersed NiO particles. These findings are in good agreement with the results reported by Mile et al.[31,32] In the case of the 20wt% Ni/ZrO_2 catalyst, the reduction maximum occurred at 420 °C, which is assigned to relatively large size NiO particles.[13, 33] The reduction profile of the 20wt% Ni/γ-Al_2O_3 sample indicated very high temperature signals one at T_{max} ~ 550 °C attributed to NiO interacted with γ-Al_2O_3 and the high temperature peak (T_{max} >800 °C) is possibly due to $NiAl_2O_4$ spinel that requires high temperature for its reduction.[34,35] However, XRD analysis did not confirm the reflections due to $NiAl_2O_4$ phase because of the superimposition of diffraction lines with that of γ-Al_2O_3

phase. The TPR results revealed that the reduction behaviour of NiO particles was strongly influenced by the type of the support.

3.3 Pyridine adsorption studies

To determine the proportion of BAS to LAS on the catalyst surface, pyridine adsorption was used in conjunction with in situ DRIFTS analysis (Fig. 3.) and the ratios of Brønsted (BAS) to Lewis acid sites (LAS) are reported in Table 1. The relative ratios of pyridine adsorbed spectral bands at 1450 cm^{-1} (Lewis acid site) and ~1540 cm^{-1} (Brønsted acid site) emphasized that all the catalysts had a higher number of LAS compared to BAS.[36] The proportion of BAS to LAS (0.38) was significantly higher on the 20wt% Ni/ZrO_2 catalyst compared to the 20wt% Ni/γ-Al_2O_3 (0.27) and 20wt% Ni/SiO_2 (0.05) catalysts (Table 1).

3.4 Catalytic hydrogenation of levulinic acid

The vapour phase hydrogenation of aqueous levulinic acid over SiO_2, γ-Al_2O_3 and ZrO_2 supported 20wt%Ni catalysts are reported in Table 2. It can be seen that the 20wt% Ni/SiO_2 catalyst exhibited better LA conversion and selectivity of GVL compared to the 20wt% Ni/γ-Al_2O_3 and 20wt% Ni/ZrO_2 catalysts. The low conversion of LA over the 20wt% Ni/ZrO_2 catalyst may have been partly due to larger Ni particles and also due to lower Ni dispersion of the catalyst.

The 20wt% Ni/SiO_2 catalyst demonstrated very good selectivity of GVL (90.6%) while the 20wt% Ni/γ-Al_2O_3 and 20wt% Ni/ZrO_2 catalysts showed moderate selectivity of 60% and 72% respectively. In addition to AL; valeric acid (VA), methyl tetra hydro furan (MTHF), 1,4-pentanediol and hydrocarbons such as butane, pentane are observed. Formation of AL is likely due to the rate at which AL is formed being faster than the rate at which it is hydrogenated to GVL. The hydrogenation reactivity of these samples is related to its surface Ni metal area (Table 2). Presence of VA and MTHF however indicate that either GVL had

reacted further and/or AL had undergone the ring opening (Scheme 2). Higher selectivity of AL over the 20wt% Ni/ZrO_2 catalyst is most likely due to this intermediate not undergoing further reaction to GVL where this conversion would rely on the hydrogenation activity of surface Ni. One possible reason is that the rate of hydrogenation of double bond (in AL) on the metal site (Ni) seems to be very high on the 20wt% Ni/SiO_2 catalyst compared to the Ni on ZrO_2 and γ-Al_2O_3 supports. Consequently, AL is undergoing ring opening to produce VA, MTHF and HCs. Another reason may presumably due to the conversion of GVL to VA, MTHF and hydrocarbons, since both the 20wt% Ni/γ-Al_2O_3 and 20wt% Ni/ZrO_2 catalysts exhibited higher number of Brønsted acid sites.

The difference in selectivity of GVL, VA and MTHF is explained in terms of variation in the nature and type of (Brønsted and/or Lewis) acid sites present on the catalyst surface. The sample (20wt% Ni/SiO_2) with lower ratio of Brønsted to Lewis acid sites (Table 1) demonstrated lower selectivity of VA and MTHF, while both the 20wt% Ni/γ-Al_2O_3 and 20wt% Ni/ZrO_2 catalysts had relatively higher BAS/LAS ratio, exhibited high selectivity of GVL ring opening products.[24] The cyclisation of LA to AL is initiated by Lewis acid sites present on the catalyst surface.[23] Presence of a significantly high ratio of BAS/LAS on the 20wt% Ni/ZrO_2 and 20wt% Ni/γ-Al_2O_3 catalysts; the rate of ring opening of either AL and/or GVL to form VA is higher; as a result decrease in GVL selectivity was observed over both the catalysts (Table 2).

4. Discussion

The product distribution is strongly influenced by the type of acid sites (Brønsted and/or Lewis) as well as their strength on the catalyst surface. A detailed investigation is carried out using two different probe molecules while co-feeding along with the aqueous LA such as pyridine (both Brønsted and Lewis acid site blocker) and 2,6-diemthylpyridine as selective Brønsted acid site (blocker) Scheme 3.

An equimolar concentration of both pyridine (12.4 mmol) and 2,6-dimethylpyridine (12.45 mmol) were introduced in the reaction stream in (4 equal) successive pulse in separate experiments. The activity data obtained after the addition of pyridine and/or 2,6-dimethylpyridine are given in Table 3. It can be seen that, significantly lower conversion was obtained over the 20wt% Ni/SiO_2 catalyst when pyridine was fed along with aqueous LA. The conversion of LA was decreased to 9.7% from 29.9% (activity loss of ~60%) however; the GVL selectivity was marginally decreased when pyridine was co-fed over the 20wt% Ni/SiO_2 catalyst (Table 3). From this, it can be inferred that the active Ni sites are not affected by the addition of pyridine. Since the BAS/LAS ratio on the 20wt% Ni/SiO_2 catalyst is less than 0.1; it is therefore concluded that Lewis acid sites are responsible for the dehydration of LA. According to the reaction mechanism, the acid sites are crucial for the dehydration of LA to AL (1^{st} step Scheme 2). The poisoned catalyst was then regenerated by replacing the aqueous LA with air flow (~20 mL min^{-1}) at 450 °C /3h and subsequently reduced the catalyst in H_2 stream at 450 °C 30 min^{-1}. After regeneration, the sample was examined for LA hydrogenation under the similar experimental conditions (Table 3). Although the catalyst suffered a loss in LA conversion after probe addition, the catalytic activity was regained its activity after the successive treatments at 450 °C in flowing air and in diluted H_2. Quite contrast to this, no significant change in LA conversion and GVL selectivity was observed when 2,6-dimethylpyridine was co-fed with aqueous LA. Pyridine would block both the Brønsted and Lewis acid sites when the catalyst is exposed at 270 °C (Scheme 3). A drastic reduction in LA conversion indicates the dependence of Lewis sites for LA conversion to AL. On the other hand, when 2,6-dimethylpyridine was added; a marginal decrease in LA conversion implies the existence of available Lewis acid sites since the 2,6-dimethylpyridine is a selective Brønsted acid site blocker (Table 3). Therefore, it can be concluded that Brønsted acid sites are playing a vital role in the ring opening of GVL, which is further

supplemented from the pyridine adsorbed FT-IR analysis. This could be explained due to the presence of strong acid sites (Brønsted); LA chemisorption occurs strong enough to cause the ring opening of AL.[24] It is thus suggested that the 20wt% Ni/γ-Al_2O_3 and 20wt% Ni/ZrO_2 catalysts possess weak hydrogenation activity than the 20wt% Ni/SiO_2 catalyst. Finally, it can be concluded that a metal site (Ni) in a close proximity to Lewis acid site is active for the selective conversion of LA to GVL. These results suggest modification of surface properties can alter the product distribution thus the desired product selectivity can be fine tuned.

The time on stream (TOS: 15 h) analysis emphasized the long term stability of 20wt% Ni/SiO_2 catalyst (Table S3). The CHNS analysis of the used catalysts revealed that there was very low amount of carbon deposition over the 20wt% Ni/SiO_2 catalyst compared to other catalysts (Table 2). The lower activity of the 20wt% Ni/γ-Al_2O_3 and 20wt% Ni/ZrO_2 catalysts may also possibly due to the deactivation of the catalysts due to fouling agents like angelica lactone formed as an intermediate leads to coke deposition (~2%) on the catalyst surface.[19]

To understand the nature of bulk NiO; an inert support i.e. α-Al_2O_3 and 20wt% Ni/α-Al_2O_3 samples examined for LA hydrogenation at a GHSV of 1.95 mL g_{cat}^{-1} s^{-1} and the results were reported in Table 4. The α-Al_2O_3 (known as an inert material possesses neither acid nor basic sites) showed minute activity at 325 °C with 100% selectivity towards AL, while the bulk NiO demonstrated about 9.5% LA conversion with 98.8% selectivity towards GVL. On the other hand, the 20wt% Ni/α-Al_2O_3 catalyst exhibited 11.2% of LA conversion and 93.6% GVL selectivity (Table 4). To further confirm the influence of acidity type and the role of metal in this hydrogenation, CeO_2 (Lewis acidic material)[37] taken and tested in the LA hydrogenation reaction which showed about 4.4% conversion of LA with 100% selectivity of angelica lactone. This result thus emphasizes the role of Ni and the support material which is being used to disperse the active metal. We believe that the transformation of LA is occurring at the interface of the catalyst.

Therefore, we can conclude that the LA conversion is initiated by the Lewis acid sites present on the catalyst surface. A combination of surface Ni metal with adjacent Brønsted acid site on the catalyst surface leads to ring opening of either GVL and/or AL to form VA and MTHF along with hydrocarbons. As aforementioned, a Lewis site combined with nickel is suitable for the selective hydrogenation of LA to GVL. Finally, it can be concluded that Lewis acid sites in close proximity to Ni site (i.e. at interface) are responsible for dehydrocyclization of LA to form AL, followed by its hydrogenation thus produce GVL. In contrast to this Ni supported on the α-Al_2O_3 demonstrated although lower LA conversion; the reaction proceeds cyclisation followed by hydrogenation to GVL. The high intrinsic activity of the 20wt% Ni/SiO_2 catalyst may be attributed to high proportion of Lewis acid sites than the Brønsted acid sites. We also believe that a uniform distribution of Ni particles on the 20wt% Ni/SiO_2 catalyst may be another reason for selective conversion of LA to GVL (Fig. S1).

5. Conclusions

The influence of supports was assessed for Ni in the LA hydrogenation by means of different conventional support. It was found that SiO_2 support is suitable for Ni for high selectivity of γ-valerolactone. In case of other supports such as ZrO_2 and γ-Al_2O_3, the selectivity of VA and MTHF are detected at the cost of GVL formation. The 20wt% Ni/ZrO_2 and 20wt% Ni/γ-Al_2O_3 catalysts demonstrated mild hydrogenation activity consequently high selectivity of angelica lactone is observed. A high ratio of Brønsted acid sites on the 20wt% Ni/ZrO_2 and 20wt% Ni/γ-Al_2O_3 catalysts resulted in ring opening of GVL. Finally it can be concluded that the product distribution can be tuned to get the desired fuel additive (GVL or VA) as the strength of surface acid-base sites regulate the selectivity in the hydrogenation of levulinic acid.

Acknowledgements

VVK and GN thank RMIT, Australia for the award of fellowship; MS, CA and VK thank CSIR New Delhi for the award of fellowship. All authors acknowledge Frank Antolasic, RMMF staff, RMIT, Australia for the support during characterization.

References

[1] M. J. Climent, A. Corma, S. Iborra, *Green Chem.,* 2014, **16**, 516.

[2] J.C. S. Ruiz, D. J. Braden, R. M. West, J. A. Dumesic, *Appl. Catal. B,* 2010, **100,** 184.

[3] J. M. Bermudez, J. A. Menéndez, A. A. Romero, E. Serrano, J. G. Martinez, R. Luque, *Green Chem.,* 2015, **15**, 2786.

[4] J. Xin, D. Yan, O. Ayodele, Z. Zhang, X. Lu, S. Zhang, *Green Chem.,* 2015, **17**, 1065.

[5] P. P. Upare , J. M. Lee, Y. K. Hwang , D. W. Hwang, J. H. Lee, S. B. Halligudi, J. S. Hwang, J. S. Chang, *ChemSusChem*, 2011, **4**, 1749.

[6] P. P. Upare, Y. K. Hwang, J. M. Lee, D. W. Hwang, J. S. Chang, *Chemsuschem*, 2015, **8**, 2345.

[7] R. A. Bourne, J. G. Stevens, J. Ke, M. Poliakoff, *Chem. Comm.,* 2007, 4632.

[8] W. Luo, P. C. A. Bruijnincx, B. M. Weckhuysen, *J. Catal.*, 2014, **320**, 33.

[9] B. P. Kumar, N. Nagaraju, V. P. Kumar, K.V.R. Chary, *Catal. Today*, 2015, **250**, 209.

[10] M. Sudhakar, M. L. Kantam, V. S. Jaya, R. Kishore, K. V. Ramanujachary, A. Venugopal, *Catal. Comm.,*2014*,* **50,** 101.

[11] W. R. H. Wright, R. Palkovits, *ChemSusChem*, 2012, **5**, 1657.

[12] J. M. Tukacs, R. V. Jones, F. Darvas, G. Dibo, G. Lezsak, L. T. Mika, *RSC Adv.*, 2013, **3**, 16283.

[13] V. Mohan, V. Venkateshwarlu, C.V. Pramod, B. D. Raju, K.S.R. Rao, *Catal. Sci. Technol.*, 2014, **4**, 1253.

[14] J. Zhang, S. Wu, B. Li, H.D. Zhang, *ChemCatChem*, 2012, 4, 1230.

[15] J. Zhang, J. Chen, Y. Guo, L. Chen, *ACS Sustainable Chem. Eng.*, 2015, 3, 1708.

[16] K. Yan, J. Liao, X. Wu, X. Xie, *RSC Adv.*, 2013, 3 3853.

[17] C. M. Marrodan, P. Barbaro, *Green Chem.,* 2014, 16, 3434.

[18] S. G. Wettstein, J. Q. Bond, D. M. Alonso, H. N. Pham, A. K. Datye, J. A. Dumesic, *App. Catal. B: Environ.,* 2012, **117-118**, 321.

[19] P.P. Upare, J.M. Lee, D.W. Hwang, S.B. Halligudi, Y.K. Hwang, J.S. Chang, *J. Ind. Eng. Chem.*, 2011, **17**, 287.

[20] M. Sudhakar, V.V. Kumar, G. Naresh, M.L. Kantam, S.K. Bhargava, A. Venugopal, *App. Catal. B,* 2016, **180**, 113.

[21] P.P. Upare, M. G. Jeong, Y. K. Hwang, D. H. Kim, Y. D. Kim, D. W. Hwang, U. H. Lee, J. S. Chang, *Appl. Catal. A*, 2015, **491**, 127.

[22] V. Mohan, C. Raghavendra, C.V. Pramod, B. D. Raju, K. S. R. Rao, *RSC Adv.,* 2014, **4**, 9660.

[23] V.V. Kumar, G. Naresh, M. Sudhakar, J. Tardio, S. K. Bhargava, A. Venugopal, *App. Catal. A,* 2015, **505**, 217.

[24] K. Kon, W. Onodera, K. I. Shimizu, *Catal. Sci. Technol.*, 2014, **4**, 3227.

[25] W. Luo, U.Deka, A.M.Beale, E.R.H.V. Eck, P.C.A. Bruijnincx, B.M. Weckhuysen, *J. Catal.*, 2013, **301**, 175.

[26] W. Luo, P.C.A. Bruijnincx, B.M. Weckhuysen, *J. Catal.*, 2014, **320**, 33.

[27] A.M. Ruppert, J. Grams, M. Jedrzejczyk, J. Matrs-Michalska, N. Keller, K. Ostojska and P. Sautet, *ChemSusChem*, 2015, **8**, 1538.

[28] J. Lv, Z. Rong, Y. Wang, J. Xiu, Y. Wang, J. Qu, *RSC Adv.,* 2015, **5**, 72037.

[29] K. Shimizhu, S. Kanno, K. Kon, *Green Chem.,* 2014, **16**, 3899.

[30] R. Rodiansono, M. D. Astuti, A. Ghofur, K. C. Sembiring, *Bullet. Chem. Reaction Eng. Catal.*, 2015, **10(2)**, 192.

[31] B. Mile, D. Stirling, M. Zammitt, A. Lovell, M. Webb, *J. Catal.*, 1988, **114**, 217.

[32] J. Xiong, J. Chen, J. Zhang, *Catal. Comm.,* 2007, **8**, 345.

[33] H. S. Roh, K. Y. Koo, J. H. Jeong, Y. T. Seo, D. J. Seo, Y.-S. Seo, W. L. Yoon, S. B. Park, *Catal. Lett.*, 2007, **117**, 85.

[34] A. J. Akande, R. O. Idem, A. K. Dalai, *Appl. Catal.*, 2005, **287**, 159.

[35] F. Marino, E. Cerrella, S. Duhalde, M. Jobbagy, M. Laborde, *Int. J. Hydrogen Energy,* 1988, **23**, 1095.

[36] H. Knözinger, P. Ratnasamy, *Catal. Rev.*, 1978, **17,** 31.

[37] Y. Wang, F. Wang, Q. Song, Q. Xin, S. Xu, J. Xu, *J. Am. Chem. Soc.,* 2013, **135**, 1506.

Figure captions

Table 1 Physico chemical characteristics of the 20wt% Ni supported on SiO_2, γ-Al_2O_3, and ZrO_2 samples.

Table 2 Product distribution in the hydrogenation of LA over 20wt% Ni supported on SiO_2, ZrO_2 and γ-Al_2O_3 catalysts. Reaction conditions: 10wt% LA in H_2O, 270 °C, catalyst wt. ~ 0.05 g, H_2 = 20 cm^3 min^{-1}, GHSV = 19.5 mL s^{-1} g_{cat}^{-1}, Activity data measured after 6 h on stream

Table 3 Influence of probe addition on aqueous LA hydrogenation over 20wt% Ni/SiO_2 catalyst Reaction conditions: 10wt% aqueous LA, 270 °C; Catalyst wt.: ~0.075 g, H_2 = 20 cm^3 min^{-1}, GHSV = 9.74 mL s^{-1} g_{cat}^{-1}.

Table 4 LA hydrogenation activities over bulk NiO, α-Al_2O_3 and 20wt% Ni/α-Al_2O_3 samples; Reaction conditions: 10wt% aqueous LA, 325 °C; Catalyst wt.: ~0.5 g, H_2 = 20 cm^3 min^{-1}, GHSV = 1.95 mL s^{-1} g_{cat}^{-1}.

Scheme 1 Possible products in the catalytic hydrogenation of levulinic acid

Scheme 2 Reaction pathways during LA hydrogenation in the vapour phase

Scheme 3 Surface poisoning of Brønsted and Lewis acid sites using pyridine (both Brønsted and Lewis site blocker) and 2,6-dimethylpyridine (selective Brønsted acid sites blocker) as probes.

Fig. 1. XRD patterns of 20wt% Ni supported on (a) SiO_2, (b) γ-Al_2O_3 and (c) ZrO_2 samples reduced at 450 °C for 3 h.

Fig. 2. The H_2-TPR profiles of 20wt% Ni supported on (a) SiO_2, (b) ZrO_2 and (c) γ-Al_2O_3 catalysts.

Fig. 3. Pyridine adsorbed drift spectra of 20wt% Ni supported on (a) ZrO_2, (b) γ-Al_2O_3 and (c) SiO_2 catalysts.

Tables

Table 1 Physicochemical characteristics of the 20wt% Ni supported on SiO_2, γ-Al_2O_3 and ZrO_2 samples.

20wt%Ni supported on	BET Surface area ($m^2\ g^{-1}$)	Ni crystallite size (nm) [a]	H_2 uptake ($\mu mol/g_{cat}$) [b]	BAS/LAS ratio [c]
SiO_2	155.5	20.5	1237	0.05
γ-Al_2O_3	108.8	21.4	1308	0.27
ZrO_2	23.5	37.8	1204	0.38

[a]Calculated from XRD spectra using Scherrer equation w.r.t Ni(111) plane
[b]Obtained from H_2-TPR analysis; calibrated with Ag_2O TPR
[c]BAS/LAS ratio obtained from pyridine adsorbed FT-IR spectra

Table 2 Product distribution in the hydrogenation of LA over 20wt% Ni supported on SiO_2, ZrO_2 and γ-Al_2O_3 catalysts. Reaction conditions: 10wt% LA in H_2O, 270 °C, catalyst wt. ~ 0.05 g, H_2 = 20 cm^3 min^{-1}, GHSV = 19.5 mL s^{-1} g_{cat}^{-1}, Activity data measured after 6 h on stream

20wt% Ni on	$\%X_{LA}$	%Selectivity					CO uptake (μmol g_{cat}^{-1})[b]	S_{Ni} (m^2/g_{Ni})[c]	TOF_{GVL} (s^{-1})[d]	Carbon (%)[e]
		GVL	AL	VA	MTHF	Others[a]				
SiO_2	15.7	90.6	1.0	0.4	3.9	2.9	74.8	14.6	1.82	0.52
ZrO_2	3.5	60.2	16.9	15.8	2.4	4.7	39.3	7.7	0.52	2.57
γ-Al_2O_3	10.7	71.9	4.2	6.6	8.2	9.0	56.5	11.1	1.32	2.28

[a] 1,4-pentanediol, pentane, butane, CO_2.
[b] CO uptakes measured from pulse chemisorption
[c] Ni metal surface areas calculated from CO uptakes
[d] Rate/CO uptake
[e] Obtained from CHNS analysis of catalysts recovered after 15 h on stream

Table 3 Influence of probe addition on aqueous LA hydrogenation over 20wt% Ni/SiO_2 catalyst, Reaction conditions: 10wt% aqueous LA, 270 °C; Catalyst wt.: ~0.075 g, H_2 = 20 cm^3 min^{-1}, GHSV = 9.74 mL s^{-1} g_{cat}^{-1}.

LA hydrogenation reaction condition and analysis	X_{LA}	S_{GVL}	S_{others}
Without probe addition[a]	29.9	90.5	10.4
After Pyridine addition[b]	9.70	81.1	18.9
After regeneration[c]	27.8	88.8	11.2
Without probe addition[a]	35.3	92.5	7.45
After 2,6-dimethylpyridine addition[b′]	25.2	91.5	8.50
After regeneration[c′]	30.7	89.6	10.4

[a] activities over 20wt%Ni/SiO_2
[b] activities after the addition of 12.4 x 10^{-3} moles of pyridine
[c] activities after regeneration of catalyst
[b′] activities after the addition of 12.45 x 10^{-3} moles of 2,6-dimethylpyridine
[c′] activities after regeneration of catalyst

Table 4 LA hydrogenation activities over bulk NiO, α-Al_2O_3 and 20wt% Ni/α-Al_2O_3 catalysts; Reaction conditions: 10wt% aqueous LA, 325 °C; Catalyst wt.: ~ 0.5 g, H_2 = 20 cm^3 min^{-1}, GHSV = 1.95 mL s^{-1} g_{cat}^{-1}.

Catalyst	X_{LA}	S_{AL}	S_{GVL}	r_{AL} / 10^{-9} (mol g_{cat}^{-1} s^{-1})	r_{GVL} / 10^{-9} (mol g_{cat}^{-1} s^{-1})
α-Al_2O_3	0.2	100	0.0	0.98	0.0
NiO	9.5	1.7	98.8	0.79	46
20wt% Ni/α-Al_2O_3	11.2	6.4	93.6	8.60	133

Schemes

Scheme1

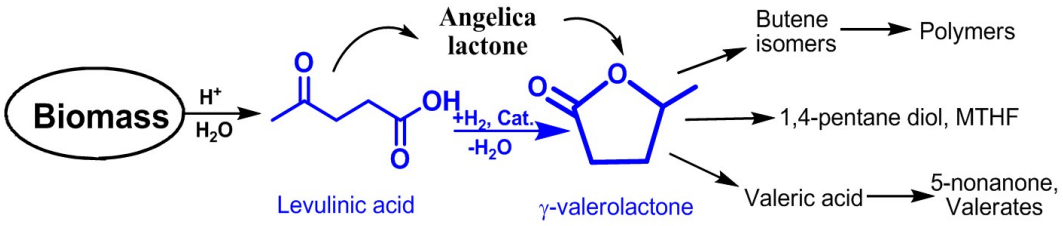

Scheme 2

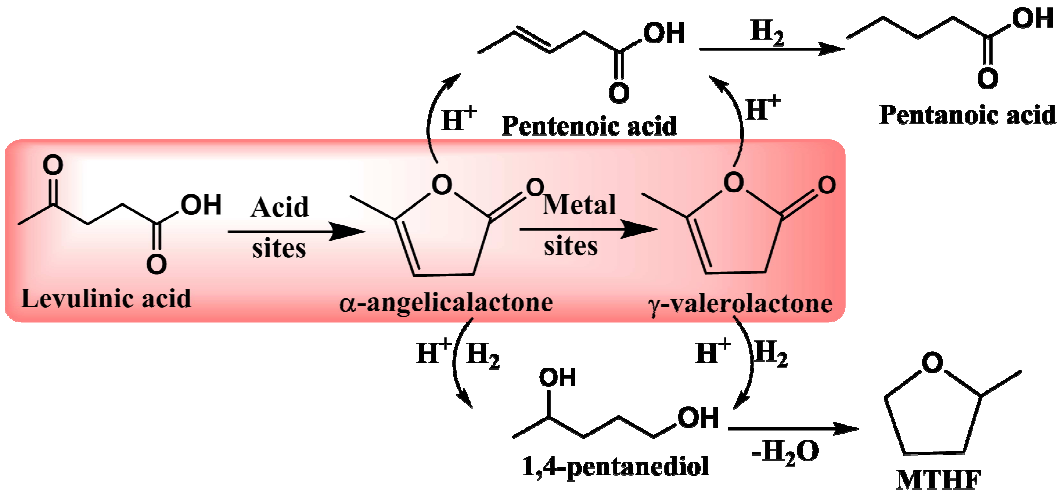

Scheme 3

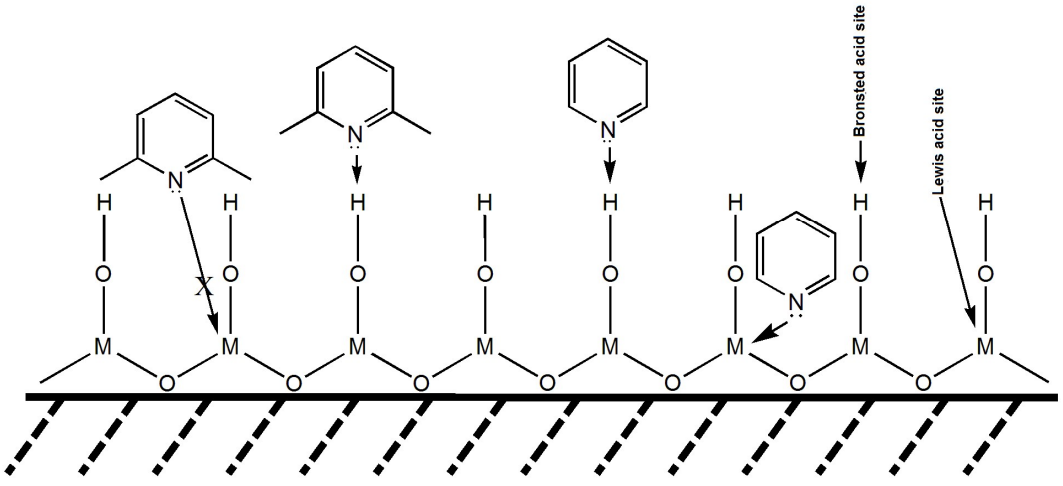

Figures

Fig. 1.

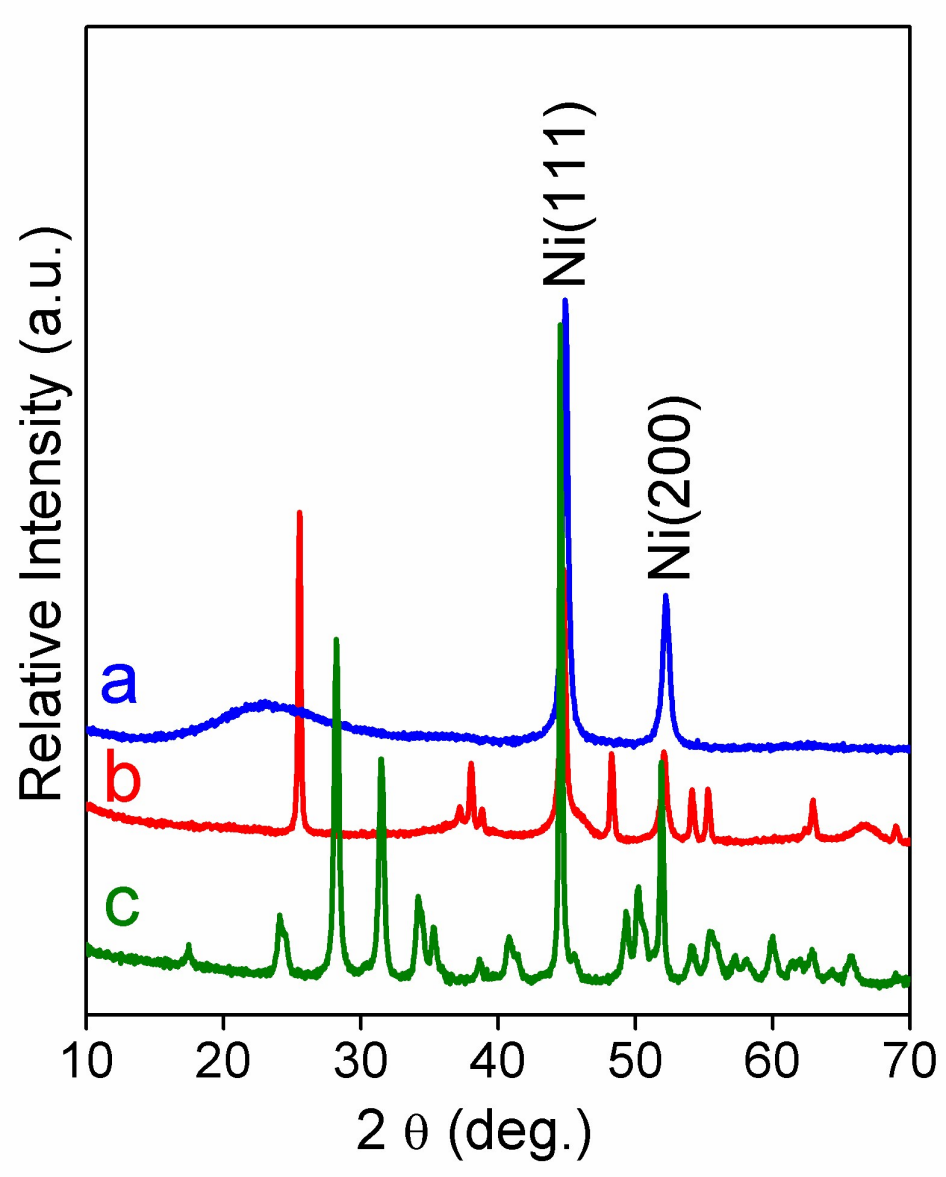

Fig. 2.

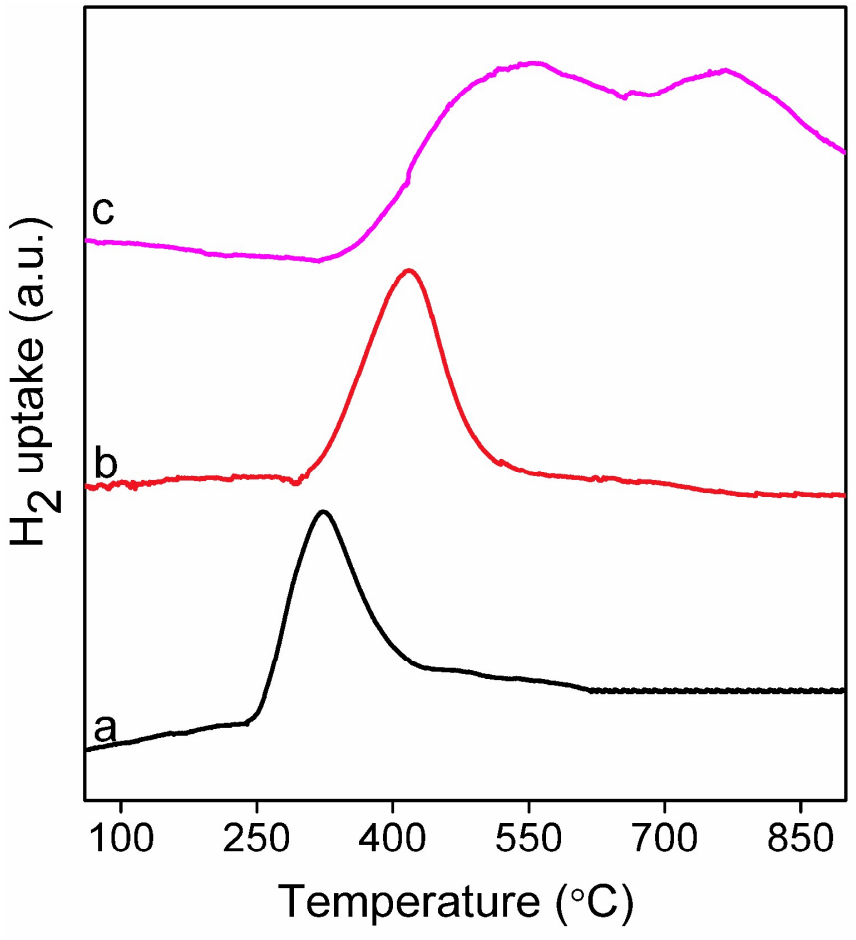

Fig. 3.